Soil Biology and Biochemistry 186 (2023) 109163

Contents lists available at ScienceDirect

Soil Biology and Biochemistry

journal homepage: www.elsevier.com/locate/soilbio

Biological nitrogen fixation in barren soils of a high-vanadium region: Roles of carbon and vanadium

Jipeng Wang [a,b], Qian Zhao [a], Yiqiu Zhong [a], Shuhao Ji [a], Guanrui Chen [a], Qingqing He [c], Yanhong Wu [d], Haijian Bing [d,*]

[a] College of Ecology and Environment, Chengdu University of Technology, 610059, Chengdu, China
[b] CAS Key Laboratory of Mountain Ecological Restoration and Bioresource Utilization and Ecological Restoration and Biodiversity Conservation Key Laboratory of Sichuan Province, Chengdu Institute of Biology, Chinese Academy of Sciences, 610041, Chengdu, China
[c] School of Emergency Management, Xihua University, 610039, Chengdu, China
[d] Key Laboratory of Mountain Surface Processes and Ecological Regulation, Institute of Mountain Hazards and Environment, Chinese Academy of Sciences, 610299, Chengdu, China

ARTICLE INFO

Keywords:
Biological nitrogen fixation
nifH gene
Carbon availability
Complementary nitrogenase
Soil vanadium
Primary succession

ABSTRACT

Free-living nitrogen fixation (FLNF) is a vital source of nitrogen for the initiation and development of ecosystems on bare lands. This process is catalyzed by the enzyme nitrogenase and is energy intensive. Of the three nitrogenase isoforms, molybdenum nitrogenase (Mo-Nase) is more efficient than its vanadium (V) and iron (Fe) counterparts at room temperature. However, the acquisition of Mo, one of the scarcest biometals in soils, represents a major resource investment for soil diazotrophs. In a vegetation restoration chronosequence developed on barren (low carbon and nitrogen) soils of a high-V region, we tested the following two hypotheses. First, the FLNF rate would be limited by the supply of energy. Second, high V availability would cut the cost of V acquisition, and it would be beneficial for diazotrophs to use V-Nase as a complement of Mo-Nase. For the soils collected along the chronosequence, the addition of a carbon cocktail remarkably stimulated the FLNF rate by relieving the energy constraint and by enriching the diazotrophic genus *Paenibacillus*. Despite the high V content in the soils, we failed to detect the *vnf* genes of V-Nase by metagenomic sequencing. Meanwhile, we observed a limited contribution of V-Nase activity to FLNF by checking the R ratio (ratio of FLNF rates measured by acetylene reduction and $^{15}N_2$ incorporation) and the production of ethane during acetylene reduction. The reason might be that the Mo availability and temperature in our study area did not reach the thresholds for the onset of V-Nase activity. Overall, our results highlight the importance of carbon supply for FLNF in barren soils, indicating that plants may effectively regulate rhizosphere diazotrophs by secreting root exudates. This may be an important mechanism by which nonnitrogen-fixing plants survive on nitrogen-poor soils at the beginning of primary succession.

1. Introduction

Nitrogen (N) limitation of primary production is widespread in terrestrial ecosystems (Elser et al., 2007; Mason et al., 2022). During the early stage of primary succession, N limitation is especially prominent due to the lack of a cycling N pool in soils (Chapin et al., 1994, 2016). Biological N fixation directly transforms atmospheric N_2 to plant-available ammonium, which is essential for the initiation and development of ecosystems on bare lands (Chapin et al., 1994; Cleveland et al., 2022; Wang et al., 2021a).

Biological N fixation is performed by nitrogenase-bearing prokaryotic microbes (diazotrophs) that are associated with plants at different levels (Reed et al., 2011). Symbiotic N fixation refers to N fixation by diazotrophs (e.g., *Rhizobia* or *Frankia*) that form a symbiotic relationship with plants in root nodules, while free-living N fixation (FLNF) includes other forms of N fixation without such a formal plant-microbe association (Reed et al., 2011; Smercina et al., 2019b). FLNF occurs ubiquitously on earth (e.g., soils, leaf surfaces, mosses and lichens) and has been recognized as an important source of N input in unmanaged ecosystems, particularly when symbiotic N-fixing plants are not the dominant species (Cleveland et al., 2022; Reed et al., 2011).

The FLNF rate in soils is typically limited by the availability of carbon

* Corresponding author.
E-mail address: hjbing@imde.ac.cn (H. Bing).

https://doi.org/10.1016/j.soilbio.2023.109163
Received 22 May 2023; Received in revised form 3 August 2023; Accepted 24 August 2023
Available online 25 August 2023

(C). Biological N fixation reactions are energy intensive, requiring at least 16 ATP to fix one N_2 molecule in vitro (Zuberer, 2021). For diazotrophs, even more energy is required to protect the oxygen (O)-sensitive nitrogenase from damage by O_2 gas (Inomura et al., 2017). The diazotrophs in root nodules are provided with photosynthates and protected from O_2 damage by the plant host, whereas the free-living diazotrophs in soils obtain energy from soil organic matter and suffer from changing environments (e.g., O_2 concentration, soil moisture and nutrient availability) (Smercina et al., 2019b). Another important regulator of FLNF is the availability of N. In N-rich environments, FLNF is suppressed, and diazotrophs lose their advantage (Dynarski and Houlton, 2018). Therefore, the availabilities of C and N, as well as substrate C:N stoichiometry, largely determine the FLNF rate (Zheng et al., 2020, 2023). In the early stage of primary succession, the suppression of FLNF by excess amounts of N is unlikely, while the limitation of the FLNF rate by C availability should be more extensive (Wang et al., 2021b). This sets the stage for nonnitrogen-fixing plant to regulate FLNF by adjusting their C input into soils (e.g., root exudates). However, more empirical evidence is required to elucidate the role of C, among other biotic and abiotic regulators, in regulating the FLNF rate during ecosystem restoration.

Nitrogenase has three isoforms depending on the metals at the active site. The molybdenum nitrogenase (Mo-Nase) is present in all diazotrophs, while the vanadium (V)- and iron (Fe)-Nases (complementary nitrogenases) have also been used by a diverse group of free-living diazotrophs to fix N (McRose et al., 2017b). The Mo-Nase has higher substrate affinity and cost less energy to reduce a N_2 molecule than the complementary nitrogenases at room temperature (Bellenger et al., 2020; Darnajoux et al., 2022). However, the acquisition of Mo may represent a major resource investment (e.g., by producing metallophores) for diazotrophs as Mo is one of the scarcest biometals in soils (Bellenger et al., 2020; McRose et al., 2017a). Diazotrophs may switch from Mo-Nase to complementary nitrogenases when Mo availability, temperature and microbial physiology do not favor the synthesis and function of Mo-Nase (Bellenger et al., 2020; Darnajoux et al., 2022; Miller and Eady, 1988). For example, under Mo limited conditions, V has been shown to support FLNF by cyanolichens (Darnajoux et al., 2014) and by a bacterium in pure cultures (Bellenger et al., 2011; Jouogo Noumsi et al., 2016). Recent studies have suggest a significant contribution of complementary nitrogenase activity to FLNF in soils, in cyanolichens and mosses of boreal and subarctic regions, and in coastal environments (Bellenger et al., 2014; Darnajoux et al., 2019; McRose et al., 2017b). While several methods (e.g., R ratio, ethane production and ISARA) have been developed for the detection of complementary nitrogenases (Bellenger et al., 2020), we are only beginning to understand the influence of V on the existence and activity of V-Nase in soils (Cleveland et al., 2022).

Here, we measured the FLNF rates in soils along a subtropical vegetation restoration chronosequence. This chronosequence was developed on barren soils covered on the top of V-titanium (Ti) magnetite tailings. The soils had low contents of C and N but high contents of V, which varied with successional stages (Long et al., 2021; Wang et al., 2023; Table S1). Thus, the chronosequence provides conditions to test the influences of C and V on FLNF at the beginning of primary succession. We hypothesized that the FLNF rate along the chronosequence would be limited by the supply of energy (C availability), but would not be suppressed by the in-situ N availability. We also hypothesized that the high V availability in our chronosequence would cut the cost of V acquisition. Considering the large resource investment required to obtain Mo from soils (Bellenger et al., 2020; McRose et al., 2017a), it may be beneficial for diazotrophs to use V-Nase as a complement of Mo-Nase, despite the lower efficiency of the V isoform. To test the hypotheses, we measured the FLNF rates using $^{15}N_2$ incorporation (rate_$^{15}N_2$) and acetylene reduction assay (rate_ARA), and examined the effects of C, Mo and V on FLNF rates. We used the ratio between rate_ARA and rate_$^{15}N_2$ (R ratio), the production of ethane during ARA, and the incidence of V-Nase genes to examine the existence of V-Nase.

2. Materials and methods

2.1. Study site and field sampling

The vegetation restoration chronosequence is located in a V–Ti magnetite tailing reservoir, southwestern China (Fig. S1). The mean annual rainfall is 860 mm which is concentrated in June to October, and the mean annual temperature is 20 °C (Long et al., 2023). Approximately every two years since the construction of the reservoir in the 1970s, the tailings were covered with subsoils excavated from the surrounding areas (thickness: ~70 cm). The dominant plant species throughout the restoration area is *Heteropogon contortus*, a local nonnitrogen-fixing grass.

We collected soil samples at 8 sites with restoration ages ranging from 5 to 40 years along the chronosequence (Fig. S1). At each site, 4 replicate 2 m × 2 m plots were set up, which were at least 10 m away from each other. Within each plot, the top 10-cm soils underneath 3 to 4 crowns of *H. contortus* were collected and pooled as one sample. The soils were sieved (≤2 mm) in the field and transported in an ice box to the laboratory. In total, 32 soil samples were collected along the chronosequence. Within 24 h after collection, 4 g of each sample were sent to Majorbio (Shanghai, China) in a dry-ice box and stored at −80 °C for molecular analyses (metagenomic sequencing, *nifH* gene sequencing and qPCR), which were used to represent the state of microbial community under "field conditions". The rest of samples were stored in a 4 °C refrigerator or oven-dried at 60 °C for the analyses of potential FLNF rate and soil properties.

Our previous study has reported the basic soil properties and nutrient contents of the collected samples (Wang et al., 2023). The soils were sandy (clay content of 3–14%) and near neutral in pH (6.3–7.4) along the chronosequence, while the total contents of organic C (SOC, 2.0–14.5 mg g^{-1}) and N (TN, 0.2–1.5 mg g^{-1}), and the extractable contents of C (EOC, 24–185 mg kg^{-1}), inorganic N (EIN, 0.6–5.1 mg kg^{-1}), and inorganic P (EIP, 0.4–3.9 mg kg^{-1}) showed considerable variations (Table S1).

2.2. FLNF rate

The 32 soil samples stored at 4 °C were adjusted to 60% water holding capacity (WHC) and pre-incubated at 25 °C for 3 days. Each sample was then divided into two portions, with one portion amended with a C cocktail which brought the final water content to 75% WHC, and the other potion with equal amount of deionized water. The two portions of samples were used to represent the state of microbial community after "2 days of incubation with and without C", respectively. The C cocktail contained equal proportions of glucose, sucrose and malic acid based on C content (Smercina et al., 2019a). The pH of the C cocktail was adjusted to 7 and the total content of the added C was 2 mg g^{-1} dry soil. After 2 days of incubation, the two portions of soils were analyzed for their potential FLNF rates using $^{15}N_2$ incorporation and ARA. Meanwhile, 2 g of each sample were sent to Majorbio for *nifH* gene sequencing and qPCR analysis.

For $^{15}N_2$ incorporation, 5 g of each sample were incubated in a 65-mL gastight Erlenmeyer flask at 25 °C for 24 h with 10% of the headspace replaced by acid-washed $^{15}N_2$ gas (99 atom%, Aladdin®, Shanghai, China), which resulted in a final headspace ^{15}N abundance of 12.5 atom %. Another 5 g of the sample, as a control, were incubated in the same manner but without the ^{15}N-labeling procedure. After incubation, the soils were oven-dried at 60 °C, and the ^{15}N abundance and N content were measured using an elemental analyzer-isotope ratio mass spectrometer (EA-IRMS, Elementar vario ISO-TOPE cube-Elementar IsoPrime 100, Germany) according to Wang et al. (2021a). The FLNF rate was calculated following equation (1) (Weaver and Danso, 1994).

$$rate\_^{15}N_2 = \frac{atom\%^{15}N_{excess} \times TN}{atom\%^{15}N_{headspace} \times t} \quad (1)$$

where $rate\_^{15}N_2$ (μg N_2 g^{-1} soil day^{-1}) is the FLNF rate measured by $^{15}N_2$ incorporation, $atom\%^{15}N_{excess}$ is the difference between atom%^{15}N values of the labeled and control samples, $atom\%^{15}N_{headspace}$ is the ^{15}N abundance of the headspace gas after the addition of $^{15}N_2$ gas (12.5%), *TN* is the total N content (μg N g^{-1} soil) of the labeled soil after incubation, and *t* is the incubation time (1 day).

For ARA, 5 g of each sample were incubated in the same manner as the $^{15}N_2$ incorporation except that 10% of the headspace was replaced by C_2H_2 gas. Soil-only and C_2H_2-only flasks were also incubated to account for endogenous C_2H_4 production and contamination in the C_2H_2 gas, respectively. The concentrations of C_2H_4 and C_2H_6 produced were analyzed using a gas chromatograph (Shimadzu GC-2010 Pro with a Porapak N column and a flame ionization detector). A gas standard (NTRM®, Chengdu, China) containing 5 and 1 ppmv of C_2H_4 and C_2H_6, respectively, was used for the quantification of the two gases. The FLNF rate (rate_ARA) was expressed as μg C_2H_4 g^{-1} soil day^{-1}. Since V-Nase typically produce C_2H_6 in addition to C_2H_4 during the C_2H_2 reduction (typically 3–8% of ethane relative to ethylene) while Mo-Nase does not produce C_2H_6 at 25 °C (Bellenger et al., 2020), the ratio between C_2H_6 and C_2H_4 was used to estimate the contribution of V-Nase to FLNF (equation (2)). We assumed a C_2H_6/C_2H_4 ratio of 3% for V-Nase to estimate the upper limit of the contribution of V-Nase activity to FLNF.

$$Contribution\_V = \frac{[C_2H_4\_V]}{[C_2H_4\_Total]} = \frac{[C_2H_6]/3\%}{[C_2H_4\_Total]} \quad (2)$$

where *Contribution_V* is the contribution of V-Nase to FLNF, $[C_2H_4\_V]$ (ppmv) is the concentration of C_2H_4 produced by V-Nase, $[C_2H_4\_Total]$ (ppmv) is the total concentration of C_2H_4 measured after incubation, $[C_2H_6]$ (ppmv) is the concentration of C_2H_4 after incubation, and 3% is the ethane produced relative to ethylene during ARA by the V-Nase.

Two replicated measurements of the potential FLNF rate (both $^{15}N_2$ incorporation and ARA) were performed for each sample. The average value of the two measurements was reported here and was used to calculate the R ratio (rate_ARA/$rate\_^{15}N_2$). The characteristic R ratio of Mo-Nase is 3–4 and that of V-Nase is ~1, which can potentially be used to discriminate the two forms of nitrogenase (Bellenger et al., 2014).

2.3. Analyses of trace metals and total P

The oven-dried soil samples were pulverized by an agate mortar and passed through a 200-mesh Nylon screen. The chemical fractions of V and Mo were analyzed by the BCR sequential extraction procedure, which was described in detail in our previous study (Bing et al., 2016). Briefly, the acid-soluble fraction was extracted with 0.11 M acetic acid, the reducible fraction was extracted with 0.5 M hydroxylammonium chloride, and the oxidizable fraction was extracted with H_2O_2 and 1.0 M ammonium acetate. The contents of the three fractions were summed as extractable V or Mo. For the analyses of the total contents of V, Mo and P, the samples were digested with a HCl–HF–HNO_3–$HClO_4$ mixture (Bing et al., 2016). The concentrations of V, Mo and P in solutions were detected by an inductively coupled plasma mass spectroscopy (ICP-MS).

2.4. Metagenomic sequencing and gene annotation

The 32 samples collected under the field conditions were used for metagenomic sequencing. Our previous study, which analyzed the genes encoding extracellular enzymes in these samples, has described the detailed methods of the soil DNA extraction and metagenomic sequencing (Wang et al., 2023). Metagenomics sequencing generated a total of 2,988,894,892 clean reads (79,956,740–110,146,870 per sample). All these clean reads were assembled into 27,097,387 contigs, and 31,869,927 open reading frames (ORFs) with an average length of 383 bp were predicted from these contigs. In the present study, we focused on the genes involved in N metabolisms (Kyoto Encyclopedia of Genes and Genomes (KEGG) PATHWAY: map00910). Gene annotation was conducted using Diamond (version 0.8.35) against the KEGG database (v94.2) with an e-value cutoff of $1e^{-5}$. Gene abundance was expressed as transcripts per million (TPM) counts, which accounts for gene length and sequencing depth when comparing the gene abundances between samples (Seyler et al., 2021). Relative abundances of the *nif* genes were also normalized by that of the prokaryotic single-copy gene *recA* to quantify the copies of genes per prokaryotic cell (Acinas et al., 2021).

2.5. Sequencing of the nifH gene

Sequencing of the *nifH* gene was performed for three batches of samples (field conditions, and 2 days of incubation without and with C; 32 samples for each batch). The primer pairs *nifH-F/nifH-R* were used for PCR amplification (Fan et al., 2019). The 20-μL PCR reaction mixture contained 4 μL of 5 × FastPfu buffer, 2 μL of 2.5 mM dNTPs, 0.8 μL of 5 μM forward primer, 0.8 μL of 5 μM reverse primer, 0.4 μL of fastPfu Polymerase, 0.2 μL of BSA, 10 ng of template DNA, and double distilled water (ddH_2O). The thermocycler was programmed with an initial denaturation at 95 °C for 3 min, followed by 40 cycles of 95 °C for 5 s, 60 °C for 30 s, 72 °C for 45 S, and followed by an extension at 72 °C for 10 min. The PCR amplicons were purified by Agarose Gel DNA purification kit (TaKaRa Bio), and triplicate PCR amplifications for each sample were conducted and pooled as a PCR product and then sequenced on the Illumina MiSeq PE300 platform (Illumina, San Diego, USA) in Majorbio.

Raw sequences were quality-filtered by fastp (version 0.19.6) and merged by FLASH (version 1.2.11). Reads with quality scores <20 or with ambiguous nucleotides were discarded. The FrameBot program was used to correct potential frame shifts caused by sequencing errors, and the sequences were then translated into amino acid sequences using the FunGene Pipeline (https://fungene.cme.msu.edu/). Only reads whose translated proteins matched the *nifH* gene-encoded protein sequence and that did not contain termination codons or chimeric sequences were retained. The remaining high-quality sequences were clustered into operational taxonomic units (OTUs) with an identity cutoff of 97% using the USEARCH11 pipeline, and the most abundant sequence from each OTU was selected as the representative sequence. The taxonomy of representative sequence was analyzed using the RDP Classifier (http://rdp.cme.msu.edu/) against the reference *nifH* sequences in FunGene database (https://fungene.cme.msu.edu/) with a confidence threshold of 0.7. In total 5,973,062 high-quality *nifH* gene sequences were generated for 96 sequenced samples (36,357–112,269 per sample), which were clustered into 4552 OTUs.

2.6. qPCR analysis of the nifH gene

The absolute abundances (copy number g^{-1} dry soil) of *nifH* gene were determined by qPCR on an ABI7300 (Applied Biosystems, CA, USA) for the same samples and using the same primer pairs as in the MiSeq sequencing. A 20-μL reaction mixture contained 10 μL of 2 × ChamQ SYBR Color qPCR Master Mix (Vazyme Biotech, Nanjing, China), 0.8 μL of each primer (5 μM), 0.4 μL of 50 × ROX Reference Dye 1, 2 μL of DNA template, and 6 μL of ddH_2O. The thermocycler was programmed with an initial denaturation at 95 °C for 3 min, followed by 40 cycles of 95 °C for 5 s, 58 °C for 30 s, and extension at 72 °C for 1 min, and followed by a final melt-curve step from 60 °C to 95 °C. To obtain the standard curve, a *nifH* gene fragment was cloned into the pMD18-T vector (2692 bp) and transferred subsequently into *Escherichia coli* cells. The plasmids containing the correct fragment length were selected and verified. The extracted plasmid DNA was used as the template to generate a standard curve. The quantification of each DNA sample was run in triplicate. The PCR amplification efficiency was 100.2% with an R^2 value of 0.999.

2.7. Metal addition experiment

To examine the effects of V and Mo on the FLNF rate and R ratio, we conducted a 28-day incubation experiment. Equal amount of the 8 samples collected at the 5- and 10-year sites were pooled as the "early-stage soil", and those collected at the 35- and 40-year sites were pooled as the "late-stage soil". The soils were pre-incubated at 25 °C, 60% WHC for 3 days, and were then amended with different solutions: C cocktail without metal (CK), C cocktail with Mo (Mo-1 and Mo-5), and C cocktail with V (V-1 and V-5). Four replicates were performed for each treatment. The C cocktail contained 700 μg C g^{-1} soil. The Mo-1 and Mo-5 treatments contained 1 and 5 μg Mo g^{-1} soil as Na_2MoO_4 in the C cocktail, respectively. The V-1 and V-5 treatments contained 1 and 5 μg V g^{-1} soil as $NaVO_3$ in the C cocktail, respectively. The solutions were mixed thoroughly into the soils at day 1, 8, 15 and 22, and the soils were incubated at 25 °C until day 28. At day 29, the soils received a further addition of a C cocktail containing 100 μg C g^{-1} soil, and their potential FLNF rates were immediately analyzed by $^{15}N_2$ incorporation and ARA.

We expected that the addition of V would favor diazotrophs containing V-Nase genes and hence enhance the activity of V-Nase, while the addition of Mo would exert the opposite effect by rendering V-Nase-mediated N fixation unnecessary. The 5 times of solution addition increased the soil water content from 60% WHC to up to 80% WHC. The C cocktail (on average 100 μg C g^{-1} soil day^{-1}) was expected to keep the diazotrophs viable during incubation and FLNF measurement (Baudoin et al., 2003).

2.8. Statistical analyses

One-way ANOVA with Tukey's post hoc test was used to test the differences among the 8 sampling sites or among the 5 treatments in the metal addition experiment. Paired-samples *t*-test was used to test the differences between the FLNF rates after 2 days of incubation without and with C. Simple linear regression was used to examine the relationship between the FLNF rates measured by $^{15}N_2$ incorporation and ARA. Pearson correlation, multiple linear regression and structural equation modeling (SEM) were used to explore the regulators of the FLNF rate (please see Supplementary methods, Tables S2 and S3, and Fig. S2 for details).

2.9. Availability of sequencing data

Sequence data associated with this study have been deposited in the Genome Sequence Archive database (GSA; https://ngdc.cncb.ac.cn/gsa/) under accession numbers CRA007329 (metagenomic sequencing) and CRA010528 (*nifH* sequencing).

3. Results

3.1. Contents of V and Mo

The content of total V (93–414 mg kg^{-1}) was lower at the 15-year site than at the other sites (Fig. 1a), while the content of extractable V (11.2–40.2 mg kg^{-1}) showed an increasing trend with site age (Fig. 1b). The content of total Mo (0.2–2.8 mg kg^{-1}) was higher at the 10-year site than at the 5-, 20- and 25-year sites (Fig. 1c), and the content of extractable Mo (0.02–0.13 mg kg^{-1}) was higher at the 40-year site than at the 10- and 20-year sites (Fig. 1d).

3.2. Abundances of nif genes

The three marker genes of Mo-Nase (*nifD*, *nifH* and *nifK*) were detected in the 32 samples collected along the chronosequence (Fig. 2), and the relative abundance of each gene was less than 0.01 copies per cell (Fig. S3). The *vnf* genes related to V-Nase were not detectable at our sequencing depth (Fig. 2).

The absolute abundance of the *nifH* gene in soils under field conditions (2.13×10^7–1.35×10^8 copies g^{-1} soil) showed an increasing trend with site age (Fig. S3). This trend was maintained for the samples that experienced 4-°C storage and 2-day incubation without C, although the gene abundance significantly decreased (Figs. S3 and S4). The absolute abundance of the *nifH* gene in the samples that experienced 2 days of incubation with C was not different among site ages (Fig. S3), and the addition of C did not lead to a significant change in *nifH* gene copy number (Fig. S4).

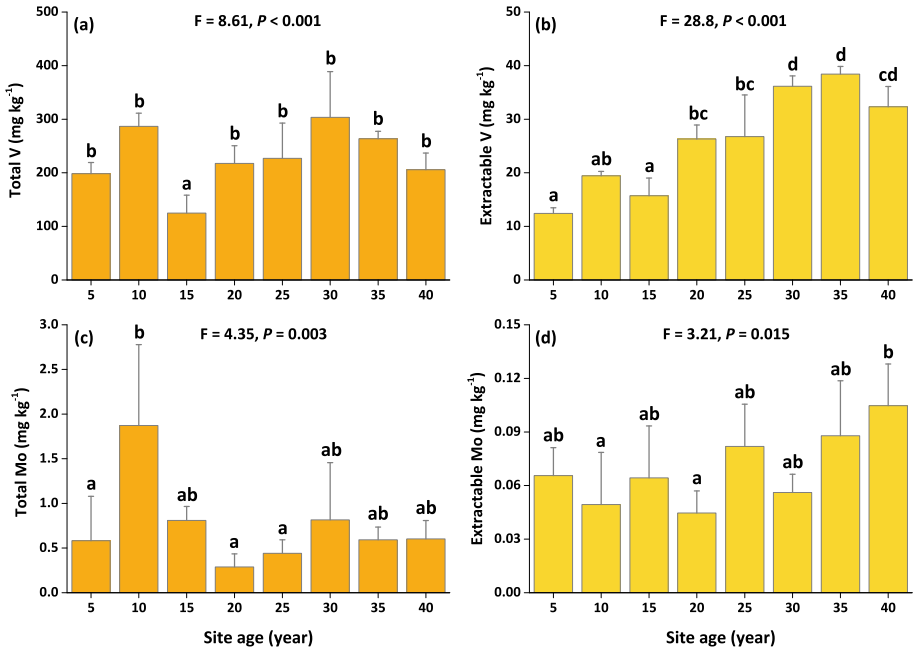

Fig. 1. Total and extractable contents of vanadium (V) and molybdenum (Mo) in soils along the vegetation restoration chronosequence. Data are presented as mean + SD (n = 4 for each treatment). Different lowercase letters indicate significant differences between sites.

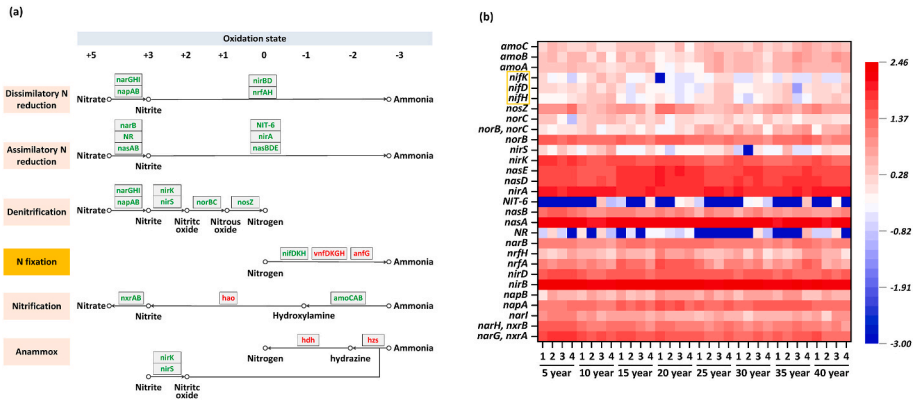

Fig. 2. Relative abundances of the genes involved in nitrogen metabolism for the 32 samples collected along the vegetation restoration chronosequence. (a): Genes marked in green were detected in metagenomic sequencing, whereas genes marked in red were undetectable at our sequencing depth. (b): heatmap of the relative gene abundances (lg-transformed) of the detectable genes in panel (a), which were expressed as $\log_{10}$(TPM + 0.001) to account for TPM (transcripts per million) values of 0 in certain samples.

3.3. Community composition of diazotrophs

The diazotrophic community was dominated by Proteobacteria (relative abundance of 79 ± 17%, mean ± SD) and an unclassified phylum (16 ± 16%) for samples under field conditions (Fig. 3a). The dominance of the two phyla was maintained in samples that experienced a 2-day incubation (Fig. 3b and c). The relative abundance of Firmicutes, which was nearly undetectable in samples under field conditions (0.04 ± 0.05%, Fig. 3a) or incubated without C (0.02 ± 0.03%, Fig. 3b), substantially increased after 2 days of incubation with C (11 ± 19%, Fig. 3c). Nearly all of the Firmicutes species (99 ± 4%) in the C-amended samples were from a single genus, *Paenibacillus* (Fig. S5).

3.4. FLNF rate and R ratio

Along the chronosequence, the FLNF rate was low or undetectable for the samples incubated for 2 days without C (0.002 ± 0.003 μg N_2 g^{-1} soil day^{-1}), while it significantly increased after the addition of C (1.18 ± 1.12 μg N_2 g^{-1} soil day^{-1}) (Fig. 4a). With the addition of C, the FLNF rate measured by $^{15}N_2$ incorporation was higher at the 10-, 30-, 35- and 40-year sites than at the 5-year site (Fig. 4b), which was consistent with the rate measured by ARA (Fig. 4c and d). The FLNF rate ($^{15}N_2$ incorporation, with C) was positively related to the contents of SOC and EIP and the relative abundance of Firmicutes, with 69% of its variation explained by the SEM (Fig. 4e and S6, Tables S2 and S3). The R ratio (0.7–17.2) did not differ among sites (Fig. 4f) and was not related to the V or Mo content in soils (Fig. S7).

For samples in the 28-day incubation experiment, the addition of V or Mo did not significantly change the FLNF rate or R ratio, except that the addition of 1 μg Mo g^{-1} soil per week increased the rate_ARA of the late-stage soil (Fig. 5).

3.5. C_2H_6 production during ARA

The production of C_2H_6 was detected in 3 of the 32 samples after 2 days of incubation with C and was detected in 7 of the 40 samples subjected to 28 days of metal treatment (Fig. S8). The C_2H_6/C_2H_4 percentages (0–0.22%) corresponded to up to a 7.4% contribution of V-Nase to the FLNF rate, assuming that V-Nase produced 3% of C_2H_6 relative to C_2H_4 during C_2H_2 reduction (Fig. S8). The production of C_2H_6 was not affected by the V content in soils or by the addition of exogenous V (Fig. S8).

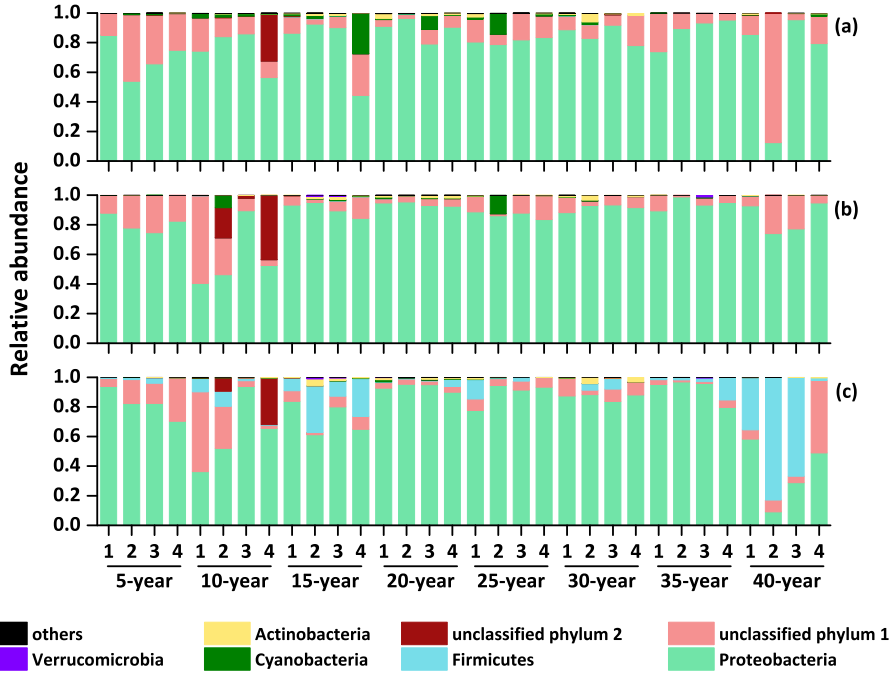

Fig. 3. Community composition of the diazotrophs along the vegetation restoration chronosequence at the phylum level. (a): field conditions, (b): after 2 days of incubation without C, (c): after 2 days of incubation with C.

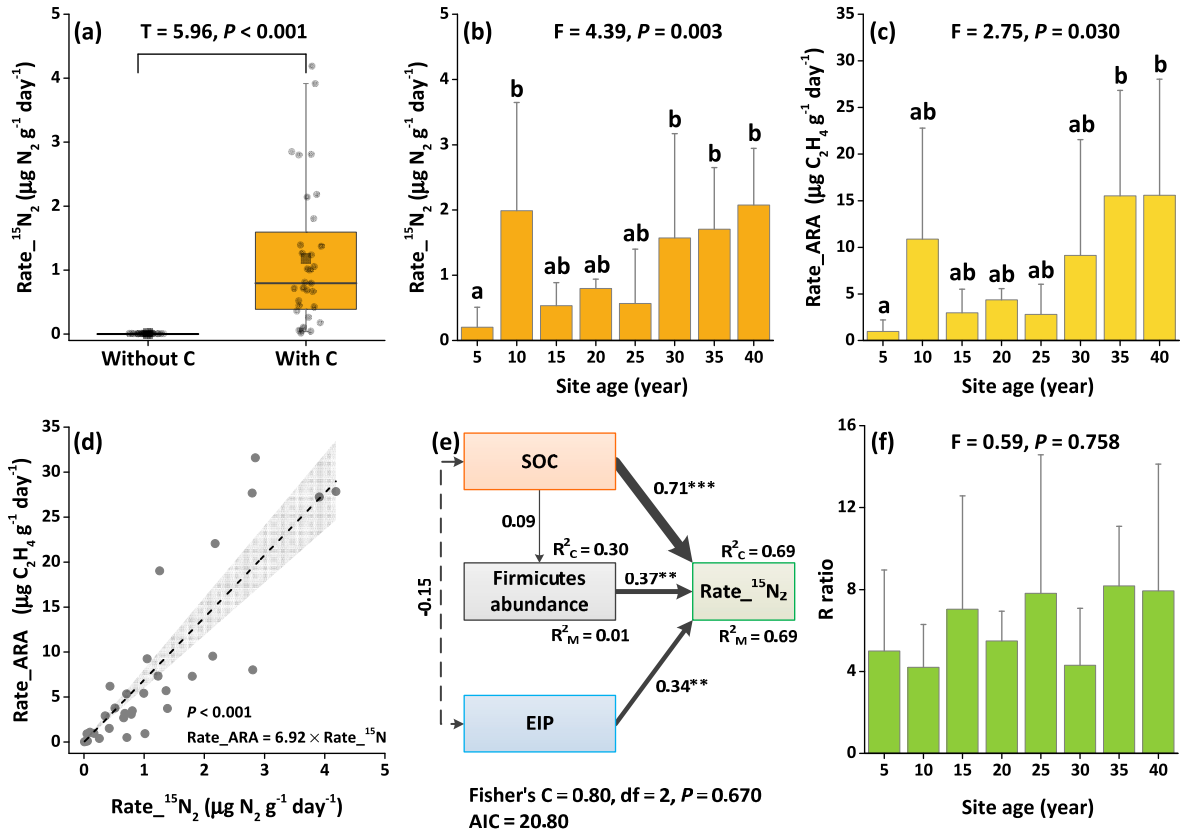

Fig. 4. FLNF rate and its regulators along the vegetation restoration chronosequence. (a): FLNF rates ($^{15}N_2$ incorporation) measured after 2 days of incubation with and without C. The line and square inside the box represent the median and mean values, respectively; the upper and lower edges of the box represent the upper and lower quartiles, respectively; and the whisker represents the 5–95% range. (b) and (c): FLNF rates (after 2 days of incubation with C) measured by $^{15}N_2$ incorporation and ARA, respectively. Data are presented as mean + SD (n = 4 for each site). Different lowercase letters indicate significant differences between sites. (d): Relationship between FLNF rates measured by $^{15}N_2$ incorporation (b) and ARA (c). (e): Structural equation modeling of the FLNF rates ($^{15}N_2$ incorporation, 2 days of incubation with C). The dashed arrows indicate correlative relationships and the solid arrows indicate causal relationships. Numbers adjacent to the arrows are standardized path coefficients and the arrow width is proportional to the path coefficient. (f): R ratio calculated using the FLNF rates measured by $^{15}N_2$ incorporation (b) and ARA (c). FLNF: free-living nitrogen fixation, ARA: acetylene reduction assay. SOC: soil organic carbon, EIP: inorganic P extracted by 0.5-M $NaHCO_3$, R^2_C: conditional R^2, the proportion of variance explained by the fixed and random effects, R^2_M: marginal R^2, the proportion of variance explained by the fixed effects.

4. Discussion

4.1. Limitation of FLNF by C availability

Our findings highlight the importance of C in regulating the FLNF rate, as has been previously reported in pure cultures and under field conditions (Smercina et al., 2019b; Zheng et al., 2023). The FLNF rates along the chronosequence were extremely low or undetectable when labile C was not added, while they significantly increased after the addition of a C cocktail containing 2 mg C g^{-1} soil (Fig. 4a). The C cocktail (glucose, sucrose and malic acid) is energy sources of a diverse array of diazotrophs (Smercina et al., 2019a), indicating that the FLNF along our chronosequence were limited by the supply of energy. This is further supported by the positive relationship between EIP and FLNF rate (Fig. 4e), as P is required for the synthesis of ATP which provides energy for the nitrogenase reaction (Vitousek et al., 2002). On the other hand, in line with a recent meta-analysis (Zheng et al., 2023), we found no sign that the C-stimulated FLNF rate was suppressed by the in-situ N availability in terms of both content and stoichiometry (Fig. 4e, Tables S2 and S3), probably due to the low N availability (total N < 0.2%) in our study area (Table S1). In fact, increasing N availability in this range may even promote FLNF by relieving the N limitation of diazotrophs (Groß et al., 2022; Reed et al., 2011). These results support our first hypothesis and were consistent with our findings in N-limited postglacial ecosystems, where the availability of C was the most important regulator of the heterotrophic FLNF rate (Wang et al., 2021b). Our C cocktail resembled root exudates, which contain low molecular weight sugars and organic acids as the main constituents (Dietz et al., 2020). Therefore, root exudates may effectively simulate rhizosphere FLNF in a similar manner and thus contribute to a mutually beneficial relationship between plants and free-living diazotrophs. This may be an important pathway by which nonnitrogen-fixing plants acquire N to survive on N-poor soils at the beginning of primary succession, in addition to other pathways such as acquiring N from cryptogamic covers or from neighboring nitrogen-fixing plants (Chapin et al., 1994; Knelman et al., 2021; Wang et al., 2021a).

We noticed that SOC was the most important regulator of the FLNF rate even after the addition of the C cocktail (Fig. 4e and S6). Since the C limitation of diazotrophs was relieved by exogenous C supply, SOC probably did not promote FLNF by acting as an energy source. It is also unlikely that SOC indirectly regulates FLNF by altering *nifH* gene abundance. First, when *nifH* gene copy number was included in the SEM, its direct effect on the FLNF rate was not significant (Fig. S2). Second, *nifH* gene copy number did not change significantly after the addition of the C cocktail (Fig. S4). The lack of a significant correlation between *nifH* gene abundance and FLNF rate has also been reported in previous

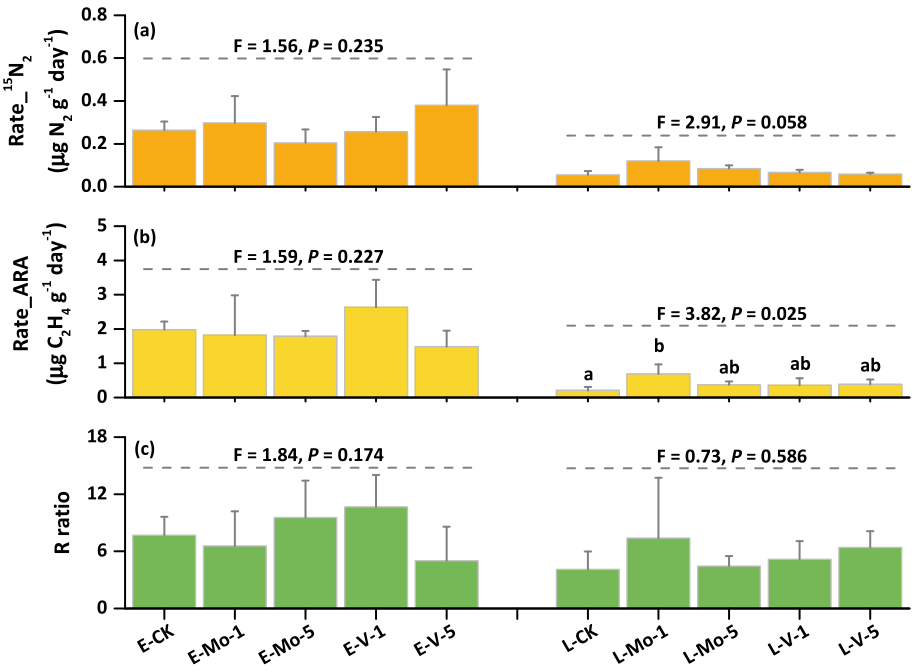

Fig. 5. FLNF rates (a and b) and R ratios (c) for the samples subjected to 28 days of metal addition. (a): FLNF rates measured by $^{15}N_2$ incorporation, (b): FLNF rates measured by ARA. E: early-stage soil, pooled samples from the 5- and 10-year sites; L: late-stage soil, pooled samples from the 35- and 40-year sites. CK: control; Mo-1 and Mo-5: additions of 1 and 5 μg g^{-1} Mo every week for 4 weeks, respectively; V-1 and V-5: additions of 1 and 5 μg g^{-1} V every week for 4 weeks, respectively. FLNF: free-living nitrogen fixation, ARA: acetylene reduction assay. Data are presented as mean + SD (n = 4 for each treatment). Different lowercase letters indicate significant differences between treatments.

studies (Brankatschk et al., 2011; Groß et al., 2022; Wang et al., 2021b)), suggesting that the expression of nitrogenase genes is tightly regulated by the surrounding environment (Dixon and Kahn, 2004). Another possible explanation may be that the diazotrophs in soils with high SOC content are more responsive to the addition of labile C (i.e., quick transition from dormancy to high-level expression of nitrogenase genes). This speculation requires testing by inspecting nitrogenase gene expression at the transcriptional level, although the significant influence of SOC on diazotrophic composition hints that some taxa were under the selection pressure of SOC (Fig. S6).

The C cocktail led to a substantial increase in the relative abundance of the phylum Firmicutes (Fig. 3), which promoted the FLNF rate (Fig. 4e). The Firmicutes in the C-amended soils was almost entirely composed of a single genus, *Paenibacillus* (Fig. S5). The genus *Paenibacillus* is typically enriched in the rhizosphere or inside plant roots, of which over 20 species can fix N (Grady et al., 2016). Strains from this genus are plant growth-promoting rhizobacteria (PGPR) and have been used as biofertilizers (Grady et al., 2016; Langendries and Goormachtig, 2021). Considering that the effects of the C cocktail on community composition occurred within 2 days and were highly repeatable in our samples (Fig. 3), it is reasonable to infer that root exudates may also stimulate FLNF by effectively enriching diazotrophic rhizobacteria.

4.2. Limited contribution of V-Nase to FLNF

The soil V contents along our chronosequence (93–414 mg kg^{-1}; Fig. 1) were in the upper range of global soil V contents (average of 97 mg kg^{-1} in the upper crust; Gustafsson, 2019). The extractable V content significantly increased with the successional stage due to continuous atmospheric deposition (Fig. 1; Long et al., 2021). Nonetheless, we failed to verify the existence of V-Nase in our study area, which is inconsistent with our second hypothesis. First, metagenomic sequencing demonstrated that the *nif* genes (Mo-Nase) and other genes associated with N metabolism were widespread along the chronosequence, but did not find sequences that could be annotated to the *vnf* genes (V-Nase) (Fig. 2). However, we cannot preclude the possibility that the sequencing depth of this study was not enough to detect the *vnf* genes that were extremely low in abundance (please see *Materials and methods* for sequencing depth).

Second, the R ratio was not affected by the soil V content. The mean R ratios were closer to the characteristic R ratio of Mo-Nase (3–4) than that of V-Nase (~1) (Figs. 4 and 5; Bellenger et al., 2020). The high R values observed in the present study are within the range reported in previous studies (Barron et al., 2009; Bellenger et al., 2014, 2020; Soper et al., 2021) and imply the dominance of Mo-Nase in our study area. However, we cannot preclude the possibility that the slow dissolution kinetics of the $^{15}N_2$ gas in our soils (>70% WHC) led to underestimation of the FLNF rate measured by $^{15}N_2$ incorporation (and thus overestimation of the R ratio; Mohr et al., 2010; Soper et al., 2021). In addition, the wide range of R ratios (0.7–17.2) in our study area encompassed the theoretical range of V-Nase. Therefore, instead of using the absolute R ratio as an indicator of V-Nase-dependent FLNF, we checked if soil V content negatively affected the R ratio. Neither soil V content nor the addition of exogenous V or Mo affected the R ratio or FLNF rate (Fig. 4e and 5 and S7), still indicating a nonsignificant contribution of V-Nase to FLNF.

Third, the production of C_2H_6 during ARA was low or undetectable and was not related to the soil V content or exogenous addition of V or Mo. We did not detect C_2H_6 in ARA for 62 of the 72 samples (32 samples after 2 days of incubation with C + 40 samples after 28 days of metal treatment) in the present study (Fig. S8). Assuming the C_2H_6/C_2H_4 ratio to be 3% for V-Nase, the upper limit of the contribution of V-Nase to FLNF was 7.4% (Fig. S8), much lower than that in cyanolichens of boreal areas (conservative estimation of 20–50%; Darnajoux et al., 2019). It should be noted that there were some samples with low FLNF rates that probably hindered accurate quantification of the produced C_2H_6. Nonetheless, 17 samples exhibited C_2H_4 concentrations larger than 200 ppmv (210–1760 ppmv) (Fig. S8). That is, even as low as 5% of contribution from V-Nase will produce C_2H_6 concentrations in the ppmv level (>0.3 ppmv), which can be reliably detected by our gas chromatograph (detection limit of 0.06 ppmv). However, we did not detect C_2H_6 in the 17 samples during ARA (Fig. S8).

Because Fe-Nase has a similar low characteristic R ratio of ~0.5 as the V-Nase and produces C_2H_6 at room temperature (Bellenger et al., 2020), the high R ratios (Figs. 4 and 5) and low C_2H_6 production (Fig. S8), as well as the lack of the *anf* gene for Fe-Nase (Fig. 2), also preclude a significant contribution of Fe-Nase to FLNF. Thus, it is likely Mo-Nase was the only dominant nitrogenase along the chronosequence.

Two reasons may account for the lack of significant V-Nase-dependent FLNF in our study area. First, the diazotrophs were probably not

severely limited by Mo. Although the threshold of Mo limitation in mineral soils remains unclear, the total Mo contents (0.2–2.8 mg kg^{-1}; Fig. 1) in our soils were larger than the putative Mo-limitation thresholds of tropical leaf litter and high-latitude cyanolichens (~0.2 and 0.25 mg kg^{-1}, respectively; Darnajoux et al., 2019; Reed et al., 2013). The near-neutral pH and low C content also restricted the complexation of Mo by iron oxides or soil organic matter, which is conducive to a high portion of available Mo (Table S1; Barron et al., 2009). In line with the potentially high Mo availability, the FLNF rates were not related to total or extractable Mo contents (32 samples, after 2 days of incubation with C; Tables S2 and S3). The late-stage soil showed signs of Mo limitation to the FLNF rate in the 28-day metal addition experiment (Fig. 5b), while this potential Mo limitation may not be strong enough to induce a switch to V-Nase-dependent FLNF. Second, low temperature (<20 °C) is required for V-Nase to function more effectively than Mo-Nase (Darnajoux et al., 2022). The mean annual temperature in our study area (20 °C) and the incubation temperature (25 °C) for FLNF measurement may be too high for the onset of the V-Nase activity. Therefore, high V content alone probably cannot induce a switch from Mo-Nase-to V-Nase-dependent FLNF. The Mo and temperature thresholds, which remain to be revealed in natural ecosystems, might also be reached to activate V-Nase.

4.3. Caveats associated with the incubation experiment

Although our incubation experiment allowed testing the effects of C and metal availability without interference from other variables, the incubation conditions differed from natural environments. First, the soil water content was kept relatively constant (70–80% WHC) during incubation, while the in-situ soil moisture can vary significantly as 90% of the precipitation occurred between June to October (Long et al., 2023). Because water content and the O_2 concentration that covaries with it are important regulators of FLNF (Smercina et al., 2019a), the impacts of root exudates and metal availability on FLNF rate in the field may be less straightforward than those observed here. Second, the addition of a C cocktail caused the accumulation of CO_2 in the flask during the 24-h gas-tight FLNF measurement, which can be more than 10-fold of the concentration in ambient atmosphere (Fig. S9). Therefore, our results should be interpreted with caution and should be tested under field conditions.

5. Conclusions

Our results highlight the importance of C supply for FLNF in barren soils. Exogenous C promoted FLNF probably by supplying energy for this process and by enriching certain taxa of diazotrophs (e.g., *Paenibacillus*). Considering the large proportion of photosynthetic C that enters the rhizosphere in the form of root exudates, this may be an important mechanism by which nonnitrogen-fixing plants acquire N at the beginning of primary succession. The lack of evidence supporting the existence of V-Nase in our study area suggests that high V content alone cannot induce a switch from Mo-Nase- to V-Nase-dependent FLNF. The thresholds of Mo and temperature for V-Nase-dependent FLNF remain to be clarified under field conditions. To further verify the roles of C and V in FLNF, the expression of both Mo- and V-Nase genes needs to be examined at the transcriptional level. More reliable methods (e.g., ISARA) are also required to quantify the contribution of V-Nase to FLNF.

Declaration of competing interest

The authors declare that they have no known competing financial interests or personal relationships that could have appeared to influence the work reported in this paper.

Data availability

Data will be made available on request.

Acknowledgements

This work is supported by National Natural Science Foundation of China (42107281 and 41701288), Sichuan Science and Technology Program (2021YJ0391), and CAS “Light of West China” Program.

Appendix A. Supplementary data

Supplementary data to this article can be found online at https://doi.org/10.1016/j.soilbio.2023.109163.

References

Acinas, S.G., Sánchez, P., Salazar, G., Cornejo-Castillo, F.M., Sebastián, M., Logares, R., Royo-Llonch, M., Paoli, L., Sunagawa, S., Hingamp, P., et al., 2021. Deep ocean metagenomes provide insight into the metabolic architecture of bathypelagic microbial communities. Communications Biology 4, 604.

Barron, A.R., Wurzburger, N., Bellenger, J.P., Wright, S.J., Kraepiel, A.M., Hedin, L.O., 2009. Molybdenum limitation of asymbiotic nitrogen fixation in tropical forest soils. Nature Geoscience 2, 42–45.

Baudoin, E., Benizri, E., Guckert, A., 2003. Impact of artificial root exudates on the bacterial community structure in bulk soil and maize rhizosphere. Soil Biology and Biochemistry 35, 1183–1192.

Bellenger, J.P., Darnajoux, R., Zhang, X., Kraepiel, A.M.L., 2020. Biological nitrogen fixation by alternative nitrogenases in terrestrial ecosystems: a review. Biogeochemistry 149, 53–73.

Bellenger, J.P., Wichard, T., Xu, Y., Kraepiel, A.M.L., 2011. Essential metals for nitrogen fixation in a free-living N2-fixing bacterium: chelation, homeostasis and high use efficiency. Environmental Microbiology 13, 1395–1411.

Bellenger, J.P., Xu, Y., Zhang, X., Morel, F.M.M., Kraepiel, A.M.L., 2014. Possible contribution of alternative nitrogenases to nitrogen fixation by asymbiotic N_2-fixing bacteria in soils. Soil Biology and Biochemistry 69, 413–420.

Bing, H., Wu, Y., Zhou, J., Liang, J., Wang, J., Yang, Z., 2016. Mobility and eco-risk of trace metals in soils at the Hailuogou Glacier foreland in eastern Tibetan Plateau. Environmental Science and Pollution Research 23 (6), 5721–5732.

Brankatschk, R., Towe, S., Kleineidam, K., Schloter, M., Zeyer, J., 2011. Abundances and potential activities of nitrogen cycling microbial communities along a chronosequence of a glacier forefield. ISME Journal 5, 1025–1037.

Chapin, F.S., Conway, A.J., Johnstone, J.F., Hollingsworth, T.N., Hollingsworth, J., 2016. Absence of net long-term successional facilitation by alder in a boreal Alaska floodplain. Ecology 97, 2986–2997.

Chapin, F.S., Walker, L.R., Fastie, C.L., Sharman, L.C., 1994. Mechanisms of primary succession following deglaciation at Glacier Bay, Alaska. Ecological Monographs 64, 149–175.

Cleveland, C.C., Reis, C.R.G., Perakis, S.S., Dynarski, K.A., Batterman, S.A., Crews, T.E., Gei, M., Gundale, M.J., Menge, D.N.L., Peoples, M.B., et al., 2022. Exploring the role of cryptic nitrogen fixers in terrestrial ecosystems: a frontier in nitrogen cycling research. Ecosystems 25, 1653–1669.

Darnajoux, R., Bradley, R., Bellenger, J.P., 2022. In vivo temperature dependency of molybdenum and vanadium nitrogenase activity in the heterocystous cyanobacteria anabaena variabilis. Environmental Science & Technology 56, 2760–2769.

Darnajoux, R., Constantin, J., Miadlikowska, J., Lutzoni, F., Bellenger, J.P., 2014. Is vanadium a biometal for boreal cyanolichens? New Phytologist 202, 765–771.

Darnajoux, R., Magain, N., Renaudin, M., Lutzoni, F., Bellenger, J.P., Zhang, X., 2019. Molybdenum threshold for ecosystem scale alternative vanadium nitrogenase activity in boreal forests. Proceedings of the National Academy of Sciences 116 (49), 24682.

Dietz, S., Herz, K., Gorzolka, K., Jandt, U., Bruelheide, H., Scheel, D., 2020. Root exudate composition of grass and forb species in natural grasslands. Scientific Reports 10, 10691.

Dixon, R., Kahn, D., 2004. Genetic regulation of biological nitrogen fixation. Nature Reviews Microbiology 2 (8), 621–631.

Dynarski, K.A., Houlton, B.Z., 2018. Nutrient limitation of terrestrial free-living nitrogen fixation. New Phytologist 217, 1050–1061.

Elser, J.J., Bracken, M.E., Cleland, E.E., Gruner, D.S., Harpole, W.S., Hillebrand, H., Ngai, J.T., Seabloom, E.W., Shurin, J.B., Smith, J.E., 2007. Global analysis of nitrogen and phosphorus limitation of primary producers in freshwater, marine and terrestrial ecosystems. Ecology Letters 10, 1135–1142.

Fan, K., Delgado-Baquerizo, M., Guo, X., Wang, D., Wu, Y., Zhu, M., Yu, W., Yao, H., Zhu, Y.-g., Chu, H., 2019. Suppressed N fixation and diazotrophs after four decades of fertilization. Microbiome 7, 143.

Grady, E.N., MacDonald, J., Liu, L., Richman, A., Yuan, Z.-C., 2016. Current knowledge and perspectives of *Paenibacillus*: a review. Microbial Cell Factories 15, 203.

Groß, C., Hossen, S., Hartmann, H., Noll, M., Borken, W., 2022. Biological nitrogen fixation and nifH gene abundance in deadwood of 13 different tree species. Biogeochemistry 161, 353–371.

Gustafsson, J.P., 2019. Vanadium geochemistry in the biogeosphere–speciation, solid-solution interactions, and ecotoxicity. Applied Geochemistry 102, 1–25.
Inomura, K., Bragg, J., Follows, M.J., 2017. A quantitative analysis of the direct and indirect costs of nitrogen fixation: a model based on *Azotobacter vinelandii*. ISME Journal 11, 166–175.
Jouogo Noumsi, C., Pourhassan, N., Darnajoux, R., Deicke, M., Wichard, T., Burrus, V., Bellenger, J.-P., 2016. Effect of organic matter on nitrogenase metal cofactors homeostasis in Azotobacter vinelandii under diazotrophic conditions. Environmental Microbiology Reports 8 (1), 76–84.
Knelman, J.E., Schmidt, S.K., Graham, E.B., 2021. Cyanobacteria in early soil development of deglaciated forefields: dominance of non-heterocytous filamentous cyanobacteria and phosphorus limitation of N-fixing Nostocales. Soil Biology and Biochemistry 154, 108127.
Langendries, S., Goormachtig, S., 2021. *Paenibacillus polymyxa*, a Jack of all trades. Environmental Microbiology 23, 5659–5669.
Long, Z., Bing, H., Zhu, H., Wu, Y., 2023. Soil covering measure mitigates vanadium loss during short-term simulated rainfall in the vanadium titano-magnetite tailings reservoir. Journal of Environmental Management 330, 117201.
Long, Z., Wu, Y., Bing, H., Zhu, H., 2021. Vanadium accumulation mode of *Heteropogon contortus* and its driving factors in Majiatian tailing reservoir in Panzhihua, Southwestern China. Chemosphere 281, 130981.
Mason, R.E., Craine, J.M., Lany, N.K., Jonard, M., Ollinger, S.V., Groffman, P.M., Fulweiler, R.W., Angerer, J., Read, Q.D., Reich, P.B., et al., 2022. Evidence, causes, and consequences of declining nitrogen availability in terrestrial ecosystems. Science 376, eabh3767.
McRose, D.L., Baars, O., Morel, F.M.M., Kraepiel, A.M.L., 2017a. Siderophore production in Azotobacter vinelandii in response to Fe-, Mo- and V-limitation. Environmental Microbiology 19 (9), 3595–3605.
McRose, D.L., Zhang, X., Kraepiel, A.M.L., Morel, F.M.M., 2017b. Diversity and activity of alternative nitrogenases in sequenced Genomes and coastal environments. Frontiers in Microbiology 8, 267.
Miller, R.W., Eady, R.R., 1988. Molybdenum and vanadium nitrogenases of *Azotobacter chroococcum*. Low temperature favours N_2 reduction by vanadium nitrogenase. Biochemical Journal 256, 429–432.
Mohr, W., Großkopf, T., Wallace, D.W.R., LaRoche, J., 2010. Methodological underestimation of oceanic nitrogen fixation rates. PLoS One 5, e12583.
Reed, S.C., Cleveland, C.C., Townsend, A.R., 2011. Functional ecology of free-living nitrogen fixation: a contemporary perspective. Annual Review of Ecology Evolution and Systematics 42, 489–512.
Reed, S.C., Cleveland, C.C., Townsend, A.R., 2013. Relationships among phosphorus, molybdenum and free-living nitrogen fixation in tropical rain forests: results from observational and experimental analyses. Biogeochemistry 114, 135–147.
Seyler, L.M., Trembath-Reichert, E., Tully, B.J., Huber, J.A., 2021. Time-series transcriptomics from cold, oxic subseafloor crustal fluids reveals a motile, mixotrophic microbial community. ISME Journal 15, 1192–1206.
Smercina, D.N., Evans, S.E., Friesen, M.L., Tiemann, L.K., 2019a. Optimization of the $^{15}N_2$ incorporation and acetylene reduction methods for free-living nitrogen fixation. Plant and Soil 445, 595–611.
Smercina, D.N., Evans, S.E., Friesen, M.L., Tiemann, L.K., 2019b. To fix or not to fix: controls on free-living nitrogen fixation in the rhizosphere. Applied and Environmental Microbiology 85, e02546-02518.
Soper, F.M., Simon, C., Jauss, V., 2021. Measuring nitrogen fixation by the acetylene reduction assay (ARA): is 3 the magic ratio? Biogeochemistry 152, 345–351.
Vitousek, P.M., Cassman, K., Cleveland, C., Crews, T., Field, C.B., Grimm, N.B., Howarth, R.W., Marino, R., Martinelli, L., Rastetter, E.B., 2002. Towards an ecological understanding of biological nitrogen fixation. Biogeochemistry 57, 1–45.
Wang, J., Chen, G., Ji, S., Zhong, Y., Zhao, Q., He, Q., Wu, Y., Bing, H., 2023. Close relationship between the gene abundance and activity of soil extracellular enzyme: evidence from a vegetation restoration chronosequence. Soil Biology and Biochemistry 177, 108929.
Wang, J., He, Q., Wu, Y., Zhu, H., Sun, H., Zhou, J., Wang, D., Li, J., Bing, H., 2021a. Effects of pioneer N_2-fixing plants on the resource status and establishment of neighboring non-N_2-fixing plants in a newly formed glacier floodplain, eastern Tibetan Plateau. Plant and Soil 458, 261–276.
Wang, J., Wu, Y., Li, J., He, Q., Zhu, H., Bing, H., 2021b. Energetic supply regulates heterotrophic nitrogen fixation along a glacial chronosequence. Soil Biology and Biochemistry 108150.
Weaver, R.W., Danso, S.K.A., 1994. Dinitrogen fixation. In: Bottomley, P.S., Angle, J.S., Weaver, R.W. (Eds.), Methods of Soil Analysis: Part 2-Microbiological and Biochemical Properties. SSSA Book Series. Soil Science Society of America, Madison, WI, pp. 1019–1045.
Zheng, M., Chen, H., Li, D., Luo, Y., Mo, J., 2020. Substrate stoichiometry determines nitrogen fixation throughout succession in southern Chinese forests. Ecology Letters 23, 336–347.
Zheng, M., Xu, M., Li, D., Deng, Q., Mo, J., 2023. Negative responses of terrestrial nitrogen fixation to nitrogen addition weaken across increased soil organic carbon levels. Science of the Total Environment 877, 162965.
Zuberer, D.A., 2021. 16-Biological dinitrogen (N_2) fixation: introduction and nonsymbiotic. In: Gentry, T.J., Fuhrmann, J.J., Zuberer, D.A. (Eds.), Principles and Applications of Soil Microbiology, third ed. Elsevier, pp. 423–453.